Applicability of the hodograph method for the problem of long-scale nonlinear dynamics of a thin vortex filament near a flat boundary

V. P. Ruban*
L.D. Landau Institute for Theoretical Physics, 2 Kosygin Street, 119334 Moscow, Russia
(Received 19 February 2003; published 9 June 2003)

Hamiltonian dynamics of a thin vortex filament in an ideal incompressible fluid near a flat fixed boundary is considered under the conditions that at any point of the curve, determining the shape of the filament, the angle between tangent vector and the boundary plane is small. Also the distance from a point on the curve to the plane is small in comparison with the curvature radius. The dynamics is shown to be effectively described by a nonlinear system of two (1+1)-dimensional partial differential equations. The hodograph transformation reduces this system to a single linear differential equation of the second order with separable variables. Simple solutions of the linear equation are investigated for real values of spectral parameter λ, when the filament projection on the boundary plane has shape of a two-branch spiral or a smoothed angle, depending on the sign of λ.

DOI: 10.1103/PhysRevE.67.066301 PACS number(s): 47.15.Ki, 47.32.Cc, 47.10.+g

I. INTRODUCTION

It is a well-known fact that the solutions of equations determining the motion of a homogeneous inviscid fluid possess a remarkable property—the lines of the vorticity field are frozen in [1–4]. Mathematical reason for this is the so-called relabeling symmetry of fluids that provides necessary conditions for applicability of the Nöther theorem and results in infinite number of the conservation laws [5–11]. Due to this basic property, in an ideal hydrodynamics some flows in a considerably long time interval have the vorticity concentrated in quasi-one-dimensional structures, vortex filaments, that fill a small part of entire bulk of the fluid. The motion of vortex filaments is a very interesting problem both from theoretical and practical viewpoints, and is a classical subject of hydrodynamics (see, for instance, Refs. [3,4,10–24], and references therein for various analytical and numerical approaches to this problem). In a general case an analytical study in this field is highly complicated because of several reasons, the main of these being nonlocality and nonlinearity of governing equations of motion. A less significant trouble seems to be the necessity of some regularization procedures for the Hamiltonian functional (the total energy) of the system in the limit of ''infinitely thin'' vortex filaments, since a logarithmic divergency takes place in some observable physical quantities (for instance, in the velocity of displacement of curved pieces of the filament) as the thickness decreases. However, in few limit cases, the dynamics of a single vortex filament can turn out to be effectively integrable. A known and very interesting example of such an integrable system is a slender nonstretched vortex filament [in the boundless three-dimensional (3D) space filled by an ideal fluid] in the so-called localized induction approximation (LIA), when in the energy of the filament only logarithmically large contributions from interaction of adjacent pieces are taken into account. In this approximation, the Hamiltonian functional is simply proportional to the length of the filament, resulting in conservation of this quantity. Thus, application of the so-called Hasimoto transformation [15,25] is appropriate and reduces the problem to (1+1)-dimensional nonlinear Schrödinger equation, that is known to be integrable by the inverse scattering method [26].

In the present work, another integrable case in vortex dynamics is recognized, the long-scale motion of a thin vortex filament near a flat fixed boundary. Mathematically, the problem of a single filament in a half space is equivalent to the problem of two symmetric filaments in the boundless space, which allows us to simplify some further calculations. Our immediate purpose will be to consider the configurations of the vortex filament which satisfy the following conditions.

(a) The angle is everywhere small between the tangent vector on the curve determining the shape of the filament and the boundary plane.

(b) The distance from an arbitrary point of the curve to the plane is small in comparison with the curvature radius at the given point, but large in comparison with the thickness of the filament.

(c) The filament projection on the boundary plane does not have self-intersections or closely approaching one-to-another different pieces.

In these conditions, the system dynamics is known to be unstable (the so-called Crow instability [14]), with the instability increment directly proportional to the wave number of (some small) long-scale perturbation of the filament shape. It is a well-known fact that such a dependence of the increment is usual for a class of local (2×2) partial differential systems that can be exactly linearized by the so-called hodograph transformation [1] exchanging dependent and independent variables. This observation has served as a significant reason to look for a natural local nonlinear approximation in description of the long-scale dynamics of a vortex filament near a flat boundary and to examine the approximation for applicability of the Hodograph method. As a result, a consistent derivation of the corresponding local approximate equations of motion has been performed. Also, the fact has been demonstrated that the nonlinear partial differential sys-

*Email address: ruban@itp.ac.ru

tem for two functions ρ and ϑ determining the shape of the filament, and depending on the time moment t and on the Cartesian coordinate x is reduced by the hodograph transformation to a linear equation. Moreover, it is possible to choose a pair of new independent variables in such a manner that in the linear partial differential equation for the function $t(\rho,\vartheta)$, the coefficients will not depend on ϑ variable. For this purpose, it is convenient to define ρ variable as double distance from a filament point to the boundary plane $y=0$, while ϑ variable will be the angle between the x direction and the tangent to the filament projection on the x-z plane. Obviously, an explicit dependence of the coefficients on ϑ will be absent due to the symmetry of the system with respect to rotations in the x-z plane. Therefore, separation of the variables will be possible and most simple solutions will have the form

$$t_\lambda(\rho,\vartheta)=\mathrm{Re}\{T_\lambda(\rho)\Theta_\lambda(\vartheta)\}. \tag{1}$$

Here λ is an arbitrary complex parameter and the complex function $\Theta_\lambda(\vartheta)$ satisfies the simple equation

$$\Theta''_\lambda(\vartheta)=\lambda\Theta_\lambda(\vartheta). \tag{2}$$

To find the complex function $T_\lambda(\rho)$, it will be necessary to solve some ordinary linear differential equations of the second order with variable coefficients which will be considered later in this paper. The corresponding geometrical configurations of the vortex filament strongly depend on λ. In particular, it will be shown that the solutions (1) with real $\lambda<-1$ describe such a shape of the (moving) vortex filament that its projection on the x-z plane has two asymptotes with the angle between them $\Delta\vartheta=\pi(1-1/\sqrt{-\lambda})$, while in the case $\lambda>0$ the projection has the shape of a two-branch spiral (see the figures).

This paper is organized as follows. In Sec. II, a necessary review is given concerning the Hamiltonian formalism adopted to the problem of frozen-in vorticity, since this approach is the most clear and compact way to treat ideal flows. Then, approximate local equations of motion for a vortex filament near a flat boundary are derived. In Sec. III, we demonstrate the applicability of the hodograph method and introduce variables that are most convenient for the particular problem. Section IV is devoted to investigation of simple solutions obtained by the separation of variables in the governing linear equation.

II. LONG-SCALE LOCAL APPROXIMATION

Existence itself of the ideal-hydrodynamic solutions in the form of quasi-one-dimensional vortex structures (vortex filaments) filling just a small part of the total fluid bulk is closely connected with the freezing-in property of the vortex lines [1–13]. Mathematically, this property is expressed by the special form of the equation of motion for the divergence-free vorticity field $\mathbf{\Omega}(\boldsymbol{r},t)=\mathrm{curl}\,\boldsymbol{v}(\boldsymbol{r},t)$,

$$\mathbf{\Omega}_t=\mathrm{curl}[\boldsymbol{v}\times\mathbf{\Omega}], \tag{3}$$

where $\boldsymbol{v}(\boldsymbol{r},t)$ is the velocity field. Since in this article we consider incompressible flows, we may write

$$\boldsymbol{v}=\mathrm{curl}^{-1}\mathbf{\Omega}=\mathrm{curl}(-\Delta)^{-1}\mathbf{\Omega}, \tag{4}$$

where Δ is the 3D Laplace operator. As it is known, the action of the inverse nonlocal operator Δ^{-1} on an arbitrary function $f(\boldsymbol{r})$ is given by the following formula:

$$-\Delta^{-1}f(\boldsymbol{r})=\int G(|\boldsymbol{r}-\boldsymbol{r}_1|)f(\boldsymbol{r}_1)d\boldsymbol{r}_1, \tag{5}$$

where

$$G(r)=\frac{1}{4\pi r}$$

is the Green function of the $(-\Delta)$ operator in the boundless space. The Hamiltonian noncanonical structure [7] of the equations of an ideal incompressible hydrodynamics is based on the following relation

$$\boldsymbol{v}=\mathrm{curl}\left(\frac{\delta\mathcal{H}}{\delta\mathbf{\Omega}}\right), \tag{6}$$

where the Hamiltonian functional $\mathcal{H}\{\mathbf{\Omega}\}$ is the kinetic energy of a homogeneous incompressible fluid (with unit density) expressed through the vorticity,

$$\mathcal{H}\{\mathbf{\Omega}\}=\frac{1}{2}\int\mathbf{\Omega}\cdot(-\Delta)^{-1}\mathbf{\Omega}d\boldsymbol{r}. \tag{7}$$

Our approach to investigation of the vortex filament motion is based on the representation of the ideal homogeneous fluid flows in terms of the frozen-in vortex lines, as described, for instance, in Refs. [10–13]. The special form (3) of the equation of motion allows us to express the vorticity field $\mathbf{\Omega}(\boldsymbol{r},t)$ in a self-consistent manner through the shape of the vortex lines (the so-called formalism of vortex lines),

$$\mathbf{\Omega}(\boldsymbol{r},t)=\int_{\mathcal{N}}d^2\nu\oint\delta(\boldsymbol{r}-\boldsymbol{R}(\nu,\xi,t))\boldsymbol{R}_\xi(\nu,\xi,t)d\xi, \tag{8}$$

where $\delta(\cdots)$ is the 3D δ-function, $\mathcal{N}$ is some 2D manifold of labels enumerating the vortex lines ($\mathcal{N}$ is determined by topological properties of a particular flow), $\nu\in\mathcal{N}$ is a label of an individual vortex line, and ξ is an arbitrary longitudinal parameter along the line. What is important is that the dynamics of the line shape $\boldsymbol{R}(\nu,\xi,t)=(X(\nu,\xi,t),Y(\nu,\xi,t),Z(\nu,\xi,t))$ is determined by the variational principle

$$\delta\left[\int\mathcal{L}dt\right]\Big/\delta\boldsymbol{R}(\nu,\xi,t)=0,$$

with the Lagrangian of the form

$$\mathcal{L}=\int_{\mathcal{N}}d^2\nu\oint([\boldsymbol{R}_\xi\times\boldsymbol{R}_t]\cdot\boldsymbol{D}(\boldsymbol{R}))d\xi-\mathcal{H}\{\mathbf{\Omega}\{\boldsymbol{R}\}\}, \tag{9}$$

where the vector function $\boldsymbol{D}(\boldsymbol{R})$ in the case of incompressible flows must satisfy the condition

$$(\nabla_{\boldsymbol{R}}\cdot\boldsymbol{D}(\boldsymbol{R}))=1. \tag{10}$$

Below, we choose $\boldsymbol{D}(\boldsymbol{R})=(0,Y,0)$.

Since we are going to deal with a very thin vortex filament, we will neglect the ν dependence of the shapes of individual vortex lines constituting the filament. By doing this step, we exclude from further consideration all the effects related to finite variable cross section and longitudinal flows inside the filament [16–20]. Thus, we consider an "infinitely narrow" vortex string with a shape $\boldsymbol{R}(\xi,t)$ and with a finite circulation $\Gamma=\int_{\mathcal{N}}d^2\nu$. However, the Hamiltonian of such a singular filament diverges logarithmically,

$$\mathcal{H}_\Gamma\{\boldsymbol{R}(\xi)\}=\frac{\Gamma^2}{8\pi}\oint\oint\frac{\boldsymbol{R}'(\xi_1)\cdot\boldsymbol{R}'(\xi_2)d\xi_1 d\xi_2}{|\boldsymbol{R}(\xi_1)-\boldsymbol{R}(\xi_2)|}\rightarrow\infty. \tag{11}$$

In order to regularize this double integral, it is possible, as a variant, to modify the Green function [13]. For example, instead of the singular function $G\propto 1/r$, one can use a smooth function such as $G_a\propto 1/\sqrt{r^2+a^2}$ or some other appropriate expression depending on a parameter a. It should be emphasized that relation $\boldsymbol{\Omega}=\operatorname{curl}\boldsymbol{v}$ is exactly satisfied only in the original nonregularized system, but in the case of a finite a it is not valid for distances of order a from the singular vortex string. Thus, the meaning of vorticity in regularized models is not so simple, but, nevertheless, relation (6) remains valid in any case. Relatively small parameter a in regularized models serves to imitate a finite width of vortex filament in the usual (nonregularized) hydrodynamics. The energy of the string turns out to be logarithmically large,

$$\mathcal{H}_\Gamma\{\boldsymbol{R}(\xi)\}\approx\frac{\Gamma^2}{4\pi}\oint|\boldsymbol{R}'(\xi)|\ln\left(\frac{\Lambda(\boldsymbol{R}(\xi))}{a}\right)d\xi, \tag{12}$$

where $\Lambda(\boldsymbol{R})$ is a typical scale depending on a given problem (in particular, the usual LIA uses $\Lambda=\text{ const}\gg a$). In our case we consider two symmetric vortex filaments in the long-scale limit, when direction of the tangent vector varies weakly on a length of order Y. For such configurations, the energy concentrated in the half space $y>0$ is approximately equal to the following expression:

$$\mathcal{H}_\Gamma\approx\frac{\Gamma^2}{4\pi}\oint\sqrt{X'^2+Y'^2+Z'^2}\ln(2Y/a)d\xi. \tag{13}$$

This local Hamiltonian is able to provide qualitatively correct dynamics of the filament down to longitudinal scales of order Y where perturbations become stable and where nonlocality comes into play. Unfortunately, we do not have a simple method to treat the Hamiltonian (13) analytically, that is why we will consider only very large scales ($L\gg Y$) and thus, suppose the slope of the tangent vector to the boundary plane to be negligibly small (this means $Y'^2\ll X'^2+Z'^2$). Then, choosing a longitudinal parameter ξ as simply the Cartesian coordinate x, we have the following approximate Lagrangian:

$$\mathcal{L}\approx\Gamma\int\left\{-Y\dot{Z}-\frac{\Gamma}{4\pi}\sqrt{1+Z'^2}\ln(2Y/a)\right\}dx, \tag{14}$$

where the functions Y and Z depend on x and t, $\dot{Z}\equiv\partial_t Z$ and $Z'\equiv\partial_x Z$. Having neglected the term Y'^2 under the square root, we sacrifice the correct behavior of perturbations with wavelengths of the order of Y, but instead we obtain an exactly solvable system, as it will be shown below.

Let us say a few words about geometrical meaning of the second term in right-hand side of the expression (14). Since we study the very long-scale limit, locally the flow under consideration looks almost like a two-dimensional flow with a small vortex at the distance Y from the straight boundary, and the expression $(\Gamma^2/4\pi)\ln(2Y/a)$ is just the energy of such a 2D flow per unit length in the third (longitudinal) direction, while the multiplier $\sqrt{1+Z'^2}dx$ gives the arc-length element in the longitudinal direction.

Now, for simplicity, we take new time and length scales to satisfy $a=1$ and $\Gamma/2\pi=1$. After that we introduce new quantities $\rho(x,t)=2Y(x,t)$ and $\mu(x,t)=\partial_x Z(x,t)$, and also the function

$$H(\rho,\mu)=F(\rho)\sqrt{1+\mu^2}, \tag{15}$$

where

$$F(\rho)=\ln\rho. \tag{16}$$

The corresponding equations of motion then can be written in the following remarkable general form:

$$\mu=\partial_x Z, \tag{17}$$

$$\partial_t\rho+\partial_x H_\mu(\rho,\mu)=0, \tag{18}$$

$$\partial_t Z+H_\rho(\rho,\mu)=0. \tag{19}$$

More explicitly, the last two equations are

$$\rho_t+\frac{\partial}{\partial x}\left[\frac{F(\rho)Z_x}{\sqrt{1+Z_x^2}}\right]=0, \tag{20}$$

$$Z_t+F'(\rho)\sqrt{1+Z_x^2}=0. \tag{21}$$

These equations have a simple geometrical treatment. Indeed, Eq. (21) means if we consider the dynamics of the filament projection on the x-z plane, then we see an element of the projection moving in the normal to the projection tangent direction with the velocity depending only on ρ and equal to $F'(\rho)$. Simultaneously, in y direction the element of the filament moves with the velocity proportional to the x-z projection curvature multiplied by the function $F(\rho)$, as shown in Eq. (20).

It is interesting to note that an analogous consideration can also give us the long-scale Hamiltonian equations of motion for a thin vortex filament in a slab of an ideal fluid between two parallel fixed boundaries at $y=-d/2$ and $y=+d/2$. One has just to define the ρ variable by the formula $\rho=(\pi/d)y$ and make substitution $F(\rho)\mapsto F^{(\epsilon)}(\rho)$, in Eq. (15) where

$$F^{(\epsilon)}(\rho)=\ln\left(\frac{\cos\rho}{\epsilon}\right) \tag{22}$$

with a small dimensionless parameter ϵ.

III. HODOGRAPH METHOD

It is important for our consideration that any nonlinear system of the form (17)–(19) can be locally reduced to a linear equation if we take ρ and μ as new independent variables (this is known as the hodograph transformation). As interesting physical examples of systems solvable by this method, the one-dimensional gas-dynamic isentropic flows should be mentioned [1], with $H(\rho,\mu)=\rho\mu^2/2+\varepsilon(\rho)$, where ρ, μ, and $\varepsilon(\rho)$ are the gas density, gas velocity, and the internal energy density, respectively. Another example is a long-wave 1D approximation describing initial evolution of a liquid inviscid column under surface tension before the formation of drops [27]. The last case formally corresponds to $\varepsilon(\rho)\propto\rho^{1/2}$, with $\rho(x,t)$ being the cross-section area of the column.

Indeed, as from Eqs. (17) and (19) we see the relation

$$dZ=\mu\, dx-H_\rho\, dt,$$

it is convenient to introduce the auxiliary function $\chi(\rho,\mu)$,

$$\chi=Z-x\mu+tH_\rho, \tag{23}$$

in order to obtain

$$d\chi=-x\, d\mu+tH_{\rho\rho}\, d\rho+tH_{\rho\mu}\, d\mu.$$

From the above expression, we easily derive

$$t=\frac{\chi_\rho}{H_{\rho\rho}},\quad x=H_{\rho\mu}\frac{\chi_\rho}{H_{\rho\rho}}-\chi_\mu. \tag{24}$$

After that we rewrite Eq. (18) in the following form:

$$\frac{\partial(\rho,x)}{\partial(t,x)}-H_{\mu\rho}\frac{\partial(\rho,t)}{\partial(t,x)}-H_{\mu\mu}\frac{\partial(\mu,t)}{\partial(t,x)}=0$$

and multiply it by the Jacobian $\partial(t,x)/\partial(\rho,\mu)$,

$$\frac{\partial(\rho,x)}{\partial(\rho,\mu)}-H_{\mu\rho}\frac{\partial(\rho,t)}{\partial(\rho,\mu)}-H_{\mu\mu}\frac{\partial(\mu,t)}{\partial(\rho,\mu)}=0.$$

Thus, now we have

$$x_\mu=H_{\mu\rho}t_\mu-H_{\mu\mu}t_\rho. \tag{25}$$

Substitution of relations (24) into this equation and subsequent simplification give us the linear partial differential equation of the second order for the function $\chi(\rho,\mu)$,

$$(H_{\mu\mu}\chi_\rho/H_{\rho\rho})_\rho-\chi_{\mu\mu}=0. \tag{26}$$

As the function $H(\rho,\mu)$ has the special form (15), it is convenient to change variables,

$$\mu=\tan\vartheta,\quad \chi(\rho,\vartheta)=-\frac{u(\rho,\vartheta)}{\cos\vartheta}, \tag{27}$$

where ϑ is the angle in the x-z plane between x direction and the tangent to the corresponding projection of the vortex filament. As a result, the relations (23) and (24) will be rewritten in the following form

$$t=-\frac{u_\rho}{F''(\rho)}, \tag{28}$$

$$x=u_\vartheta\cos\vartheta+\left(u-\frac{F'(\rho)}{F''(\rho)}u_\rho\right)\sin\vartheta, \tag{29}$$

$$Z=u_\vartheta\sin\vartheta-\left(u-\frac{F'(\rho)}{F''(\rho)}u_\rho\right)\cos\vartheta, \tag{30}$$

and the coefficients of the linear equation for the function $u(\rho,\vartheta)$ will not depend on ϑ variable,

$$\frac{\partial}{\partial\rho}\left(\frac{F(\rho)}{F''(\rho)}u_\rho\right)-(u_{\vartheta\vartheta}+u)=0. \tag{31}$$

The same is true for the coefficients of the equation determining the function $t(\rho,\vartheta)=-u_\rho(\rho,\vartheta)/F''(\rho)$,

$$F(\rho)t_{\rho\rho}+2F'(\rho)t_\rho-F''(\rho)t_{\vartheta\vartheta}=0. \tag{32}$$

Once some particular solution of Eq. (31) is known, then further procedure consists in the following two steps.

(i) In terms of some parameter ξ find the curves of constant values of the function $t=-u_\rho(\rho,\vartheta)/F''(\rho)$. It is this point where nonlinearity comes into play, since we need to solve the nonlinear equation.

(ii) Substitute the obtained expressions $\rho=\rho(\xi,t)$ and $\vartheta=\vartheta(\xi,t)$ into Eqs. (29) and (30), and get a complete description of the filament motion, $X=X(\xi,t)$, $Z=Z(\xi,t)$, $Y=(1/2)\rho(\xi,t)$.

Thus, the long-scale local approximation (14) turns out to be integrable in the sense that it can be reduced to the *linear* equation (31). However, the function $u(\rho,\vartheta)$ is multivalued in a general case. Therefore, statement of the Cauchy problem becomes much more complicated. Besides, the functions $F(\rho)$ and $F^{(\epsilon)}(\rho)$ determined by expressions (16) and (22) result in *elliptic* linear equations as against the usual 1D gas dynamics where the corresponding equations were *hyperbolic*. Generally speaking, the ellipticity makes the Cauchy problem ill posed in the mathematical sense if initial data are not very smooth. However, in this paper we will not discuss these questions, instead in the following section we will present simple particular solutions, which within some time interval satisfy the applicability conditions for the long-scale approximation.

IV. PARTICULAR SOLUTIONS

A. Separation of the variables

We are going to consider the simplest particular solutions of Eq. (31) obtainable by separation of the variables

$$u_\lambda(\rho,\vartheta)=\mathrm{Re}\{U_\lambda(\rho)\Theta_\lambda(\vartheta)\}, \tag{33}$$

where λ is an arbitrary complex spectral parameter,

$$\lambda=(\varkappa+ik)^2, \quad k\geqslant 0, \tag{34}$$

and the function $\Theta_\lambda(\vartheta)$ contains two arbitrary complex constants C_λ^+ and C_λ^-,

$$\Theta_\lambda(\vartheta)=C_\lambda^+\exp[(\varkappa+ik)\vartheta]+C_\lambda^-\exp[-(\varkappa+ik)\vartheta]. \tag{35}$$

The motion of the vortex filament will be described by the following formulas:

$$t_\lambda=-\mathrm{Re}\left\{\frac{U_\lambda'(\rho)}{F''(\rho)}\Theta_\lambda(\vartheta)\right\}, \tag{36}$$

$$x_\lambda=\mathrm{Re}\left\{U_\lambda(\rho)\Theta_\lambda'(\vartheta)\cos\vartheta + \left(U_\lambda(\rho)-\frac{F'(\rho)}{F''(\rho)}U_\lambda'(\rho)\right)\Theta_\lambda(\vartheta)\sin\vartheta\right\}, \tag{37}$$

$$Z_\lambda=\mathrm{Re}\left\{U_\lambda(\rho)\Theta_\lambda'(\vartheta)\sin\vartheta - \left(U_\lambda(\rho)-\frac{F'(\rho)}{F''(\rho)}U_\lambda'(\rho)\right)\Theta_\lambda(\vartheta)\cos\vartheta\right\}. \tag{38}$$

The function $U_\lambda(\rho)$ must satisfy the ordinary differential equation of the second order

$$\frac{d}{d\rho}\left(\frac{F(\rho)}{F''(\rho)}U_\lambda'(\rho)\right)-(\lambda+1)U_\lambda(\rho)=0. \tag{39}$$

Let us turn a bit of attention to the special value $\lambda=-1$ of the spectral parameter, when the solution of Eq. (39) can be explicitly written for any function $F(\rho)$,

$$U_{-1}(\rho)=A_{-1}\int^\rho\frac{F''(\rho_1)d\rho_1}{F(\rho_1)}+B_{-1}, \tag{40}$$

where A_{-1} and B_{-1} are arbitrary complex constants.

At $\lambda\neq-1$, it is convenient to deal with the function

$$T_\lambda(\rho)=-\frac{U_\lambda'(\rho)}{F''(\rho)}, \tag{41}$$

which satisfies the equation

$$F(\rho)T_\lambda''(\rho)+2F'(\rho)T_\lambda'(\rho)-\lambda F''(\rho)T_\lambda(\rho)=0. \tag{42}$$

In particular, Eq. (42) is simply solvable at $\lambda=0$ (this solution describes the motion of a perfect vortex ring),

$$T_0(\rho)=A_0\int^\rho\frac{d\rho_1}{F^2(\rho_1)}+B_0. \tag{43}$$

Simple manipulations with formulas (36)–(39) allow us to rewrite the solutions in the following form

$$t_\lambda=\mathrm{Re}\{T_\lambda(\rho)\Theta_\lambda(\vartheta)\}, \tag{44}$$

$$x_\lambda=\mathrm{Re}\{(\lambda+1)^{-1}\{-[F(\rho)T_\lambda(\rho)]'\Theta_\lambda'(\vartheta)\cos\vartheta + [\lambda F'(\rho)T_\lambda(\rho)-F(\rho)T_\lambda'(\rho)]\Theta_\lambda(\vartheta)\sin\vartheta\}\}, \tag{45}$$

$$Z_\lambda=\mathrm{Re}\{(\lambda+1)^{-1}\{-[F(\rho)T_\lambda(\rho)]'\Theta_\lambda'(\vartheta)\sin\vartheta - [\lambda F'(\rho)T_\lambda(\rho)-F(\rho)T_\lambda'(\rho)]\Theta_\lambda(\vartheta)\cos\vartheta\}\}. \tag{46}$$

B. Real λ

Let us first consider real values of the spectral parameter, $\lambda\in\mathcal{R}$, and the corresponding real functions $\Theta_\lambda(\vartheta)$ and $U_\lambda(\rho)$. Since $F(\rho)>0$, $F''(\rho)<0$, we may expect the solutions $U_\lambda(\rho)$ with $\lambda\geqslant 1$ to have a large number of oscillations. In the opposite case, when $\lambda<-1$, the solutions will be a linear combination of two functions, one of them being increasing, and other decreasing. It is sufficient to know these general properties to get an impression concerning the geometrical configurations of the vortex filament described by the formulas (44)–(46). Let us take $\lambda=-k^2$ with $k>1$ and suppose the explicit dependence $T_{-k^2}(\rho)$ to be known and increasing at large ρ. For simplicity, we take $\Theta_{-k^2}(\vartheta)=\cos(k\vartheta)$ and after that resolve the relation (44) with respect to ϑ,

$$\vartheta=\pm\frac{1}{k}\arccos\left[\frac{t}{T_{-k^2}(\rho)}\right]. \tag{47}$$

Substitution of this expression into formulas (45)–(46) gives us the final form of the solutions as dependences $X_{-k^2}(\rho,t)$ and $Z_{-k^2}(\rho,t)$,

$$\begin{aligned}X_{-k^2}(\rho,t)=&\pm\frac{k^2F'(\rho)T_{-k^2}(\rho)+F(\rho)T'_{-k^2}(\rho)}{k^2-1}\left[\frac{t}{T_{-k^2}(\rho)}\right]\\&\times\sin\left(\frac{1}{k}\arccos\left[\frac{t}{T_{-k^2}(\rho)}\right]\right)\\&\mp\frac{k[F(\rho)T_{-k^2}(\rho)]'}{k^2-1}\left[1-\frac{t^2}{T^2_{-k^2}(\rho)}\right]^{1/2}\\&\times\cos\left(\frac{1}{k}\arccos\left[\frac{t}{T_{-k^2}(\rho)}\right]\right),\end{aligned} \tag{48}$$

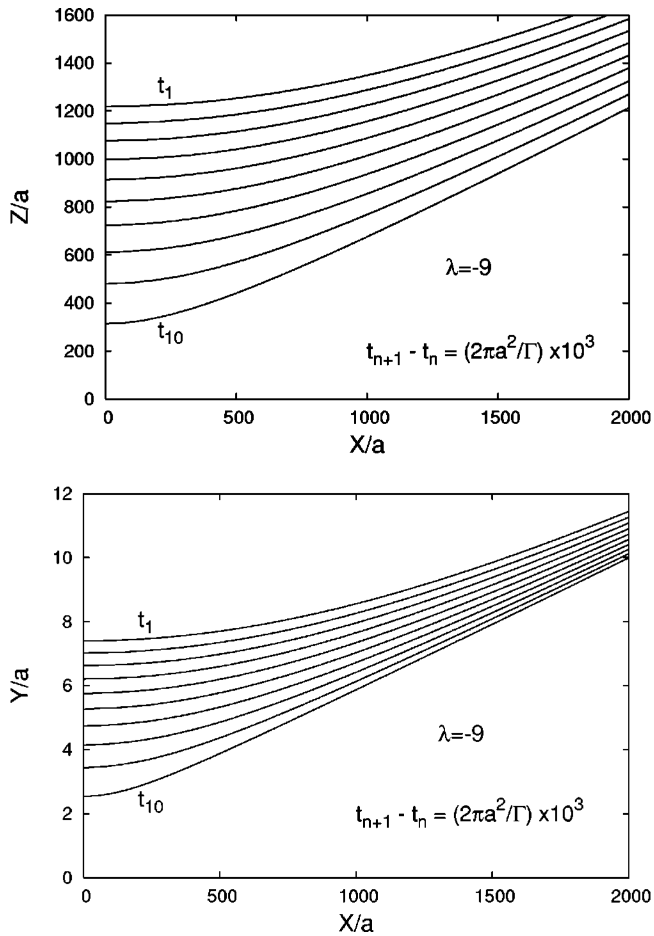

FIG. 1. Solution for $\lambda=-9$. With positive Γ the vortex filament gets closer to the wall, while for negative Γ the filament moves away from the boundary.

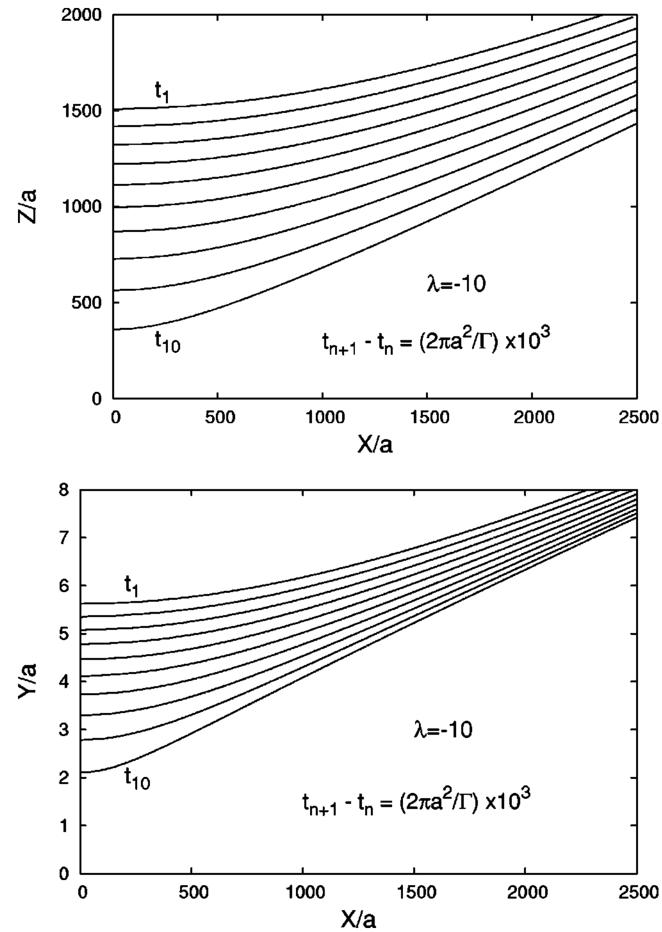

FIG. 2. Solution for $\lambda=-10$, the same time moments as in Fig. 1.

$$
\begin{aligned}
Z_{-k^2}(\rho,t) = & \mp \frac{k^2 F'(\rho) T_{-k^2}(\rho) + F(\rho) T'_{-k^2}(\rho)}{k^2-1}\left[\frac{t}{T_{-k^2}(\rho)}\right] \\
& \times \cos\left(\frac{1}{k}\arccos\left[\frac{t}{T_{-k^2}(\rho)}\right]\right) \\
& \mp \frac{k[F(\rho)T_{-k^2}(\rho)]'}{k^2-1}\left[1-\frac{t^2}{T^2_{-k^2}(\rho)}\right]^{1/2} \\
& \times \sin\left(\frac{1}{k}\arccos\left[\frac{t}{T_{-k^2}(\rho)}\right]\right).
\end{aligned} \tag{49}
$$

The ρ variable in the above expressions varies in the limits from $\rho_{min}(t)$, such that $t=T_{-k^2}(\rho_{min})$, to $+\infty$. The corresponding curve in the x-z plane is a smoothed angle $\Delta\vartheta = \pi(1-1/k)$ [see Figs. 1 and 2, where for the case $F(\rho) = \ln\rho$ the filament shape is shown at several time moments, $t_{n+1}-t_n=$ const]. Completely different form is obtained at $\lambda=\varkappa^2$, two-branch spirals (see Fig. 3). Let us take $\Theta_{\varkappa^2}(\vartheta) = \exp(\varkappa\vartheta)$. Then,

$$
\vartheta = \frac{1}{\varkappa}\ln\left[\frac{t}{T_{\varkappa^2}(\rho)}\right], \tag{50}
$$

$$
\begin{aligned}
X_{\varkappa^2}(\rho,t) = \frac{t}{T_{\varkappa^2}(\rho)}\Bigg\{ & \frac{\varkappa^2 F'(\rho) T_{\varkappa^2}(\rho) - F(\rho) T'_{\varkappa^2}(\rho)}{\varkappa^2+1} \\
& \times \sin\left(\frac{1}{\varkappa}\ln\left[\frac{t}{T_{\varkappa^2}(\rho)}\right]\right) - \frac{\varkappa[F(\rho)T_{\varkappa^2}(\rho)]'}{\varkappa^2+1} \\
& \times \cos\left(\frac{1}{\varkappa}\ln\left[\frac{t}{T_{\varkappa^2}(\rho)}\right]\right)\Bigg\},
\end{aligned} \tag{51}
$$

$$
\begin{aligned}
Z_{\varkappa^2}(\rho,t) = \frac{t}{T_{\varkappa^2}(\rho)}\Bigg\{ & -\frac{\varkappa^2 F'(\rho) T_{\varkappa^2}(\rho) - F(\rho) T'_{\varkappa^2}(\rho)}{\varkappa^2+1} \\
& \times \cos\left(\frac{1}{\varkappa}\ln\left[\frac{t}{T_{\varkappa^2}(\rho)}\right]\right) - \frac{\varkappa[F(\rho)T_{\varkappa^2}(\rho)]'}{\varkappa^2+1} \\
& \times \sin\left(\frac{1}{\varkappa}\ln\left[\frac{t}{T_{\varkappa^2}(\rho)}\right]\right)\Bigg\}.
\end{aligned} \tag{52}
$$

The variable ρ runs here between two neighbor zeros of the function $T_{\varkappa^2}(\rho)$ and approaches these values at two loga-

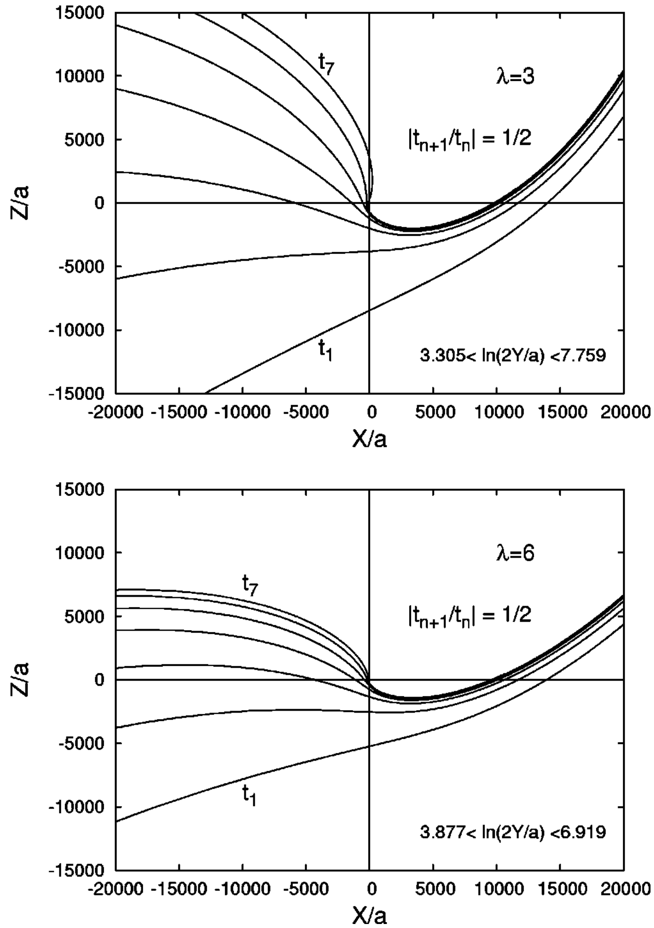

FIG. 3. Two-branch spirals. The filament projection is presented here for several negative time moments before a finite singularity, or for positive time moments after an initial singularity, depending on the direction of the vorticity.

rithmic branches of the spiral, $\rho_j^{(\varkappa)}<\rho<\rho_{j+1}^{(\varkappa)}$. It is interesting to note that the features similar to such spirals as in Fig. 3, typically develop in numerical simulations of vortex filaments (see, for example, Fig. 10 in the paper by Pumir and Siggia [16]).

C. The case $F(\rho)=\ln\rho$

For further investigation, let us substitute $F(\rho)=\ln\rho$ into Eqs. (36)–(39), and change the variable

$$q=\ln\rho.$$

As a result, we will obtain the following:

$$t_\lambda=\mathrm{Re}\{e^{q}U'_\lambda(q)\Theta_\lambda(\vartheta)\}, \tag{53}$$

$$x_\lambda=\mathrm{Re}\{U_\lambda(q)\Theta'_\lambda(\vartheta)\cos\vartheta + [U_\lambda(q)+U'_\lambda(q)]\Theta_\lambda(\vartheta)\sin\vartheta\}, \tag{54}$$

$$Z_\lambda=\mathrm{Re}\{U_\lambda(q)\Theta'_\lambda(\vartheta)\sin\vartheta - [U_\lambda(q)+U'_\lambda(q)]\Theta_\lambda(\vartheta)\cos\vartheta\}, \tag{55}$$

$$qU''_\lambda(q)+(1+q)U'_\lambda(q)+(1+\lambda)U_\lambda(q)=0. \tag{56}$$

General solution of Eq. (56) is representable by the Laplace method [28] as an arbitrary linear combination $A_\lambda I_\lambda^{\mathcal{A}}(q)+B_\lambda I_\lambda^{\mathcal{B}}(q)$ of two contour integrals in a complex plane,

$$U_\lambda(q)=\frac{A_\lambda}{2\pi i}\oint_{\mathcal{A}}\left(\frac{p}{p+1}\right)^{\lambda+1}\frac{e^{pq}dp}{p} + B_\lambda\int_{\mathcal{B}}\left(\frac{p}{p+1}\right)^{\lambda+1}\frac{e^{pq}dp}{p}. \tag{57}$$

Here, the first closed contour $\mathcal{A}$ goes around the points $p_0=0$ and $p_1=-1$. The second contour $\mathcal{B}$ is not closed, at positive q it starts at $\mathrm{Re}p=-\infty$. If $\mathrm{Re}\lambda<0$, then contour $\mathcal{B}$ ends at p_1, but if $\mathrm{Re}\lambda\geqslant 0$, then its end point will be p_0. In both cases, at the end point of the contour $\mathcal{B}$, the integrand multiplied by $p(p+1)$ tends to zero.

It is interesting to note that at the integer values of the parameter λ, the integral $I_\lambda^{\mathcal{A}}(q)$ can be expressed in terms of polynomials:

$$I_\lambda^{\mathcal{A}}(q)=\frac{1}{2\pi i}\oint_{\mathcal{A}}\left(\frac{p}{p+1}\right)^{\lambda+1}\frac{e^{pq}dp}{p} = \begin{cases}\left(1+\dfrac{d}{dq}\right)^{|\lambda|-1}\dfrac{q^{|\lambda|-1}}{(|\lambda|-1)!}, & \lambda=-1,-2,\ldots;\\[2ex] e^{-q}\left(\dfrac{d}{dq}-1\right)^{\lambda}\dfrac{q^\lambda}{\lambda!}, & \lambda=0,1,2,\ldots\,.\end{cases} \tag{58}$$

These expressions have been used to prepare Figs. 1–3, where the vortex filament shape corresponding to $U_\lambda(q)=I_\lambda^{\mathcal{A}}(q)$ is drawn for several moments of time. It is easy to see that at sufficiently large times the spirals satisfy the conditions (a), (b), and (c), which have been formulated in the Introduction. As to the angle-shaped configurations, the condition $Y'^2\ll X'^2+Z'^2$, generally speaking, is not satisfied at $q\gtrsim k^2$, since at very large q (on the asymptotes of the angle) the growth of $Y[\sim\exp(q)]$ is faster than growth of X and $Z[\sim U_{-k^2}(q)\sim q^{k^2-1}]$. Therefore, if we take a particular solution $u=U_{-k^2}(q)\cos(k\vartheta)$ separately, not as a term in a more complex linear combination, then we have to deal only with large k, and consider only the pieces of the filament where $2\ldots3\lesssim q\ll k^2$.

D. The case $F(\rho)=\rho^\alpha/\alpha$

In Ref. [13], we investigated another regularization of the Hamiltonian functional which corresponds to $F(\rho)=\rho^\alpha/\alpha$, with some small positive parameter α. That time we did not see applicability of the hodograph method and therefore, we were able to find only few particular solutions. Now it has been made clear that in this case, a simple substitution exists that reduces the problem to 2D equation $\Delta_2 f+f=0$. Thus, it becomes possible to present a very wide class of solutions of the equation

$$\rho^2 t_{\rho\rho} + 2\alpha\rho t_\rho + \alpha(1-\alpha)t_{\vartheta\vartheta} = 0 \tag{59}$$

as linear combinations of singular fundamental solutions (which are expressed through the McDonald function K_0) and regular exponential or polynomial solutions. Indeed, by the substitutions

$$\rho = e^q, \quad \vartheta = \phi\sqrt{\alpha(1-\alpha)}, \quad t = e^{(1/2-\alpha)q} f(q,\phi), \tag{60}$$

Eq. (59) is reduced to the following equation with constant: coefficients,

$$f_{qq} + f_{\phi\phi} - (1/2-\alpha)^2 f = 0. \tag{61}$$

As it is well known, the fundamental solutions of this equation have the form

$$f(q,\phi;q_0,\phi_0) = K_0\left(\left|\frac{1}{2}-\alpha\right|\sqrt{(q-q_0)^2+(\phi-\phi_0)^2}\right), \tag{62}$$

where q_0 and ϕ_0 are arbitrary parameters. Therefore, Eq. (59) has particular solutions

$$t = \rho^{1/2-\alpha} K_0\left(\left|\frac{1}{2}-\alpha\right|\sqrt{\left[\ln\frac{\rho}{\rho_0}\right]^2 + \frac{(\vartheta-\vartheta_0)^2}{\alpha(1-\alpha)}}\right). \tag{63}$$

It is interesting to note that at $\alpha = 1/2$, the system possesses a conformal symmetry. A deep reason of this symmetry is not clear yet.

As concerning separation of the variables, the function $T_\lambda(\rho)$ in Eqs. (44)–(46) is given by the expression

$$T_\lambda(\rho) = A_\lambda^+ \rho^{s_+(\lambda)} + A_\lambda^- \rho^{s_-(\lambda)}, \tag{64}$$

where $A_\lambda^\pm$ are arbitrary constants. The complex exponents $s_\pm(\lambda)$ are the roots of the quadratic equation

$$s(s-1) + 2\alpha s + \alpha(1-\alpha)\lambda = 0. \tag{65}$$

Thus,

$$s_\pm(\lambda) = 1/2 - \alpha \pm \sqrt{(1/2-\alpha)^2 - \alpha(1-\alpha)\lambda}. \tag{66}$$

It should be mentioned that the solutions presented in Ref. [13] correspond to the particular case $\alpha + s = 2$.

V. CONCLUSIONS

In this paper, an approximate exactly solvable nonlinear model has been derived to describe unstable locally quasi-2D ideal flows with a thin vortex filament near a flat boundary. The Hodograph method has been applied and some particular solutions have been analytically found by separation of variables in the governing linear partial differential equation for auxiliary function u. More general solutions $u(\rho,\vartheta)$ can be obtained as linear combinations of the terms (33) with different λ, but only in few cases will it be possible to resolve analytically the dependence $t = -u_\rho(\rho,\vartheta)/F''(\rho)$. However, this procedure can be performed numerically.

Though we derived the exactly solvable model under several restrictive simplifications, the solutions obtained in this work promise benefit in many aspects. For instance, they may serve as basic approximations in future for more advanced analytical studies that will take into account the effects of nonlocality and/or finite variable cross section of the filament, as well as surface waves in the case of free boundary.

ACKNOWLEDGMENTS

These investigations were supported by INTAS (Grant No. 00292), by RFBR, by the Russian State Program of Support of the Leading Scientific Schools, and by the Science Support Foundation, Russia.

[1] L.D. Landau and E.M. Lifshitz, *Fluid Mechanics* (Pergamon, New York, 1987) [Russian original, Nauka, Moscow, 1988].
[2] V.I. Arnold, *Mathematical Methods of Classical Mechanics*, 2nd ed. (Springer-Verlag, New York, 1989).
[3] P.G. Saffman, *Vortex Dynamics* (Cambridge University Press, Cambridge, 1992).
[4] A.J. Chorin, *Vorticity and Turbulence* (Springer-Verlag, New York, 1994).
[5] R. Salmon, Annu. Rev. Fluid Mech. **20**, 225 (1988).
[6] N. Padhye and P.J. Morrison, Plasma Phys. Rep. **22**, 869 (1996).
[7] V.E. Zakharov and E.A. Kuznetsov, Usp. Fiz. Nauk **167**, 1137 (1997) [Phys. Usp. **40**, 1087 (1997)].
[8] V.I. Ilgisonis and V.P. Lakhin, Plasma Phys. Rep. **25**, 58 (1999).
[9] V.P. Ruban, Zh. Éksp. Teor. Fiz. **116**, 563 (1999) [JETP **89**, 299 (1999)].
[10] V.P. Ruban, Phys. Rev. D **62**, 127504 (2000).
[11] V.P. Ruban, Phys. Rev. E **64**, 036305 (2001).
[12] V.P. Ruban and D.I. Podolsky, Phys. Rev. D **64**, 047503 (2001).
[13] V.P. Ruban, D.I. Podolsky, and J.J. Rasmussen, Phys. Rev. E **63**, 056306 (2001).
[14] S.C. Crow, AIAA J. **8**, 2172 (1970).
[15] H. Hasimoto, J. Fluid Mech. **51**, 477 (1972).
[16] A. Pumir and E.D. Siggia, Phys. Fluids **30**, 1606 (1987).
[17] T.S. Lungren and W.T. Ashurts, J. Fluid Mech. **200**, 283 (1989).
[18] J.S. Marshall, J. Fluid Mech. **229**, 311 (1991).
[19] A. Leonard, Phys. Fluids **6**, 765 (1994).
[20] R. Klein, O. Knio, and L. Ting, Phys. Fluids **8**, 2415 (1996).
[21] M.F. Lough, Phys. Fluids **6**, 1745 (1994).
[22] H. Zhou, Phys. Fluids **9**, 970 (1997).
[23] H. Wang, Phys. Rev. Lett. **80**, 4665 (1998).
[24] V.E. Zakharov, in *Nonlinear MHD Waves and Turbulence*, edited by T. Passot and P.L. Sulem (Springer, Berlin, 1999), Vol. 536, pp. 369–385.

[25] K. Nakayama, H. Segur, and M. Wadati, Phys. Rev. Lett. **69**, 2603 (1992).
[26] V.E. Zakharov, S.V. Manakov, S.P. Novikov, and L.P. Pitaevskii, *Theory of Solitons. The Inverse Problem Method* (Plenum, New York, 1984).
[27] J. Eggers, Rev. Mod. Phys. **69**, 865 (1997).
[28] L.D. Landau and E.M. Lifshitz, *Quantum Mechanics. Non-Relativistic Theory* (Pergamon, Oxford, 1977).